Title	Proton Induced Reactions on　Be from 4 to 6 MeV (Memorial Issue Dedicated to the Late Professor Yoshiaki Uemura)
Author(s)	Yasue, Masaharu; Ohsawa, Takao; Fujiwara, Noboru; Kakigi, Shigeru; Nguyen, D.C.; Yamashita, Sukeaki
Citation	Bulletin of the Institute for Chemical Research, Kyoto University (1974), 52(1): 177-201
Issue Date	1974-07-25
URL	http://hdl.handle.net/2433/76528
Right	
Type	Departmental Bulletin Paper
Textversion	publisher

Proton Induced Reactions on ^{9}Be from 4 to 6 MeV

Masaharu Yasue[†], Takao Ohsawa, Noboru Fujiwara,
Shigeru Kakigi, D. C. Nguyen[*],
and
Sukeaki Yamashita[**]

Excitation functions and angular distributions for the ^{9}Be(p, p)^{9}Be, ^{9}Be(p, d)^{8}Be, and ^{9}Be(p, α)^{6}Li reactions have been measured over the range of proton bombarding energies from 4.0 to 6.0 MeV. In the ^{9}Be(p, p_0)^{9}Be(g'nd), ^{9}Be(p, p_2)^{9}Be(2.43), and ^{9}Be(p, α_2)^{6}Li(3.56) reactions, a resonance has been observed at Ep=4.7 MeV, corresponding to the 10.8 MeV state in ^{10}B. The spin-parity of the 10.8 MeV state in ^{10}B has been determined to be 2^+ by the analysis of the angular distributions for the (p, p_2) and (p, α_2) reactions. In the ^{9}Be(p, α_1)^{6}Li(2.18) and ^{9}Be(p, α_2)^{6}Li(3.56) reactions, a resonance corresponding to the 11.5 MeV state of ^{10}B has been observed at Ep=5.5 MeV.

In the ^{9}Be(p, p_0)^{9}Be(g'nd) and ^{9}Be(p, α_0)^{6}Li(g'nd) reactions and in the ^{9}Be(p, p_1)^{9}Be(1.67) reaction, new resonances have been observed at Ep=4.5 MeV (Ex(^{10}B)=10.6 MeV) with a width of 200 keV and at Ep=5.1 MeV (Ex(^{10}B)=11.2 MeV) with a width of 300 keV, respectively. Besides, a gross bump with a width of about 1 MeV has been found in the ^{9}Be(p, p_0)^{9}Be(g'nd) reaction around Ep=4.5 MeV.

I. INTRODUCTION

Evidence for a singlet deuteron (d*) production, that is, the formation of a p–n pair in a $^1S_0$ state, has been reported by many authors.[1] Studies on the (p, d*) and (^{3}He, d*) reactions on light nuclei[2] revealed that the singlet deuteron is described as a single particle on the surface of the nucleus.

If so, it is expected that the excitation functions for the emission of singlet deuterons can be a probe to the study on the strength of the p–n correlation in a singlet state, *i.e.* the strength of the probability of the d* clustering in the nucleus.

As an example for the existence of the d* clustering in the nucleus, a 3.56 MeV state in ^{6}Li is mentioned. The configuration of the 3.56 MeV state of ^{6}Li is interpreted to be [α+d*] $J^\pi=0^+$; T=1 through the study on the electron scattering from ^{6}Li.[3] A ^{10}B nucleus is also an odd-odd nucleus as ^{6}Li is so, and the 8.9 MeV and 10.8 MeV states in ^{10}B are found in the excitation functions of the ^{9}Be(p, α_2)^{6}Li (3.56)· reaction by Marion.[4] If the d* correlation exists in the 8.9 MeV and 10.8 MeV states in ^{10}B, these states will be described in the configuration of a d* coupled to a ^{8}Be core. The ^{8}Be core decays into two alpha particles in the free space. Considering the structure of the 3.56 MeV state in ^{6}Li, therefore, the excited states in ^{10}B with

---

* 安江正治, 大沢孝夫, 藤原　昇, 柿木　茂, ニュエン・ダイカ : Institute for Chemical Research, Kyoto University, Kyoto.
** 山下佐明 : Nara Women's University, Nara.
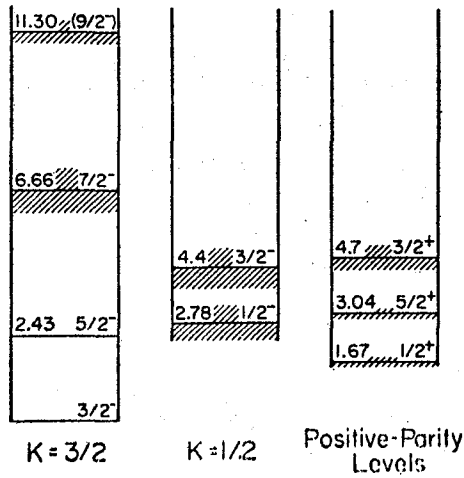† Present Address: Institute for Nuclear Study, University of Tokyo, Tokyo.

Fig. 1. Low-lying states of ^{9}Be shown as two rotational bands with $K=1/2$ and $K=3/2$ for the negative-parity states, together with the positive-parity states. Cited from Ref. 5.
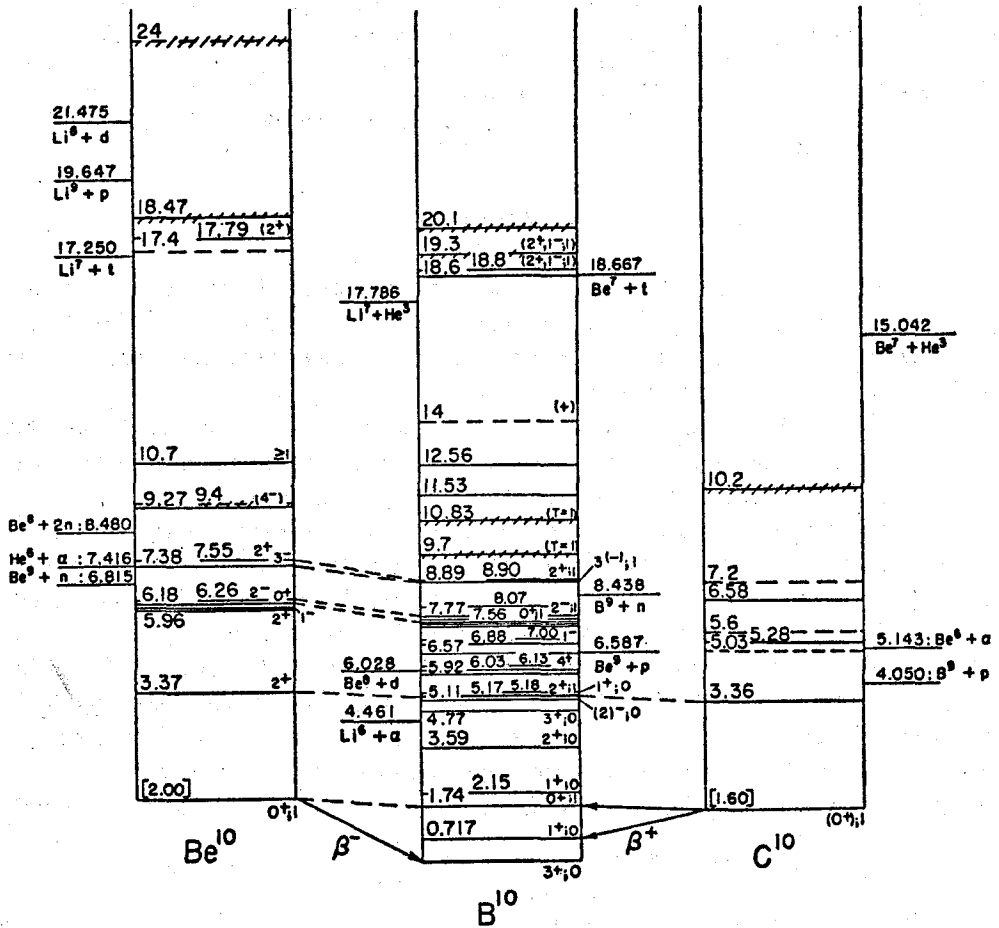

Fig. 2. The mass-10 isobaric triad. Cited from Ref. 7.

the configuration [^{8}Be+d*] will be observed in the ^{9}Be (p, α_2)^{6}Li (3.56) reaction. Hence the excitation function for the ^{9}Be (p, α_2)^{6}Li (3.56) reaction can be a probe to study the d* clustering in the ^{10}B nucleus.

Figure 1 shows the level scheme for a ^{9}Be nucleus. Negative parity states in ^{9}Be are interpreted in the strong-coupling model to a k=3/2 rotational band or a k=1/2 rotational band.[5] While, positive parity states are described in the weak-coupling model in terms of the configuration of a neutron in ls-2d shells coupled to a ^{8}Be core.[6] If the coupling between d* and ^{8}Be core is strong in the excited states of ^{10}B, the states decay into the negative parity states of ^{9}Be following an emission of a proton. While, if the coupling is weak, the states will decay into the positive parity state of ^{9}Be.

Figure 2 shows the level scheme for the mass-10 isobaric triad.[7] The 10.8 MeV state is observed in the reaction ^{9}Be (p, n)^{9}B, ^{9}Be (p, α_2)^{6}Li (3.56), and ^{10}B (e, e')^{10}B* reactions.[4, 8, 9] The 11.5 MeV state is observed in the ^{11}B (^{3}He, α)^{10}B reaction.[7]

Hitherto these high excited states have not been investigated by the proton scattering channels. As mentioned above, the ^{9}Be (p, p')^{9}Be channels give a clue to the problem whether the coupling between two particles outside of the core and the ^{8}Be core is strong or weak. Therefore, it is interesting to study these high excited states through the proton scattering channels.

In the present experiment, in order to study the structure of the 10.8 MeV and the 11.5 MeV states in ^{10}B, excitation functions and angular distributions for the proton induced reactions on ^{9}Be i.e. (p, p), (p, d), and (p, α) reactions were measured over the the range of proton energies from 4.0 MeV to 6.0 MeV, corresponding to the excitation energies in ^{10}B from 10.2 MeV to 12.0 MeV.

II. EXPERIMENTAL PROCEDURE

A proton beam from the tandem Van de Graaff accelerator of Kyoto University was brought into a 100 cm scattering chamber through an analyzing magnet. A beam defining hole of 3 mm in diameter was placed at the entrance to the scattering chamber. The beam spot at the target was about 2 by 3 mm^2. The beam energy spread was about 10 keV.

A self supporting ^{9}Be target of 35 μg/cm^2 was prepared by the vacuum evaporation method as follows.

To evaporate beryllium metal under high vacuum onto clean gass slides coated with nitro-cellulose. A tangusten boat was used to heat the beryllium for the evaporation with the electron bombarding method. The foils were then floated off the glass in an acetone bath and deposited on the target holders. Energy losses in the target are 2.2 keV for 5 MeV protons and 26 keV for 5 MeV alpha particles. The thickness of the target was calibrated with a ^{9}Be-foil of 2.53 mg/cm^2 thickness, comparing the yields for the protons elastically scattered from ^{9}Be nucleus.

Photograph 1 shows the set-up system for the detector in the scattering chamber. A detector was set on the arm and two detectors were set on the turn table. For the measuring of protons and deuterons, two silicon surface barrier detectors of 500 μm depletion depth and that of 1000 μm depth were used and Al-foils of suitable thickness were placed in front of each counter to stop alpha particles and recoil lithium ions.

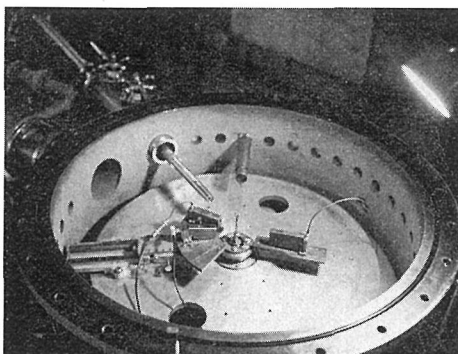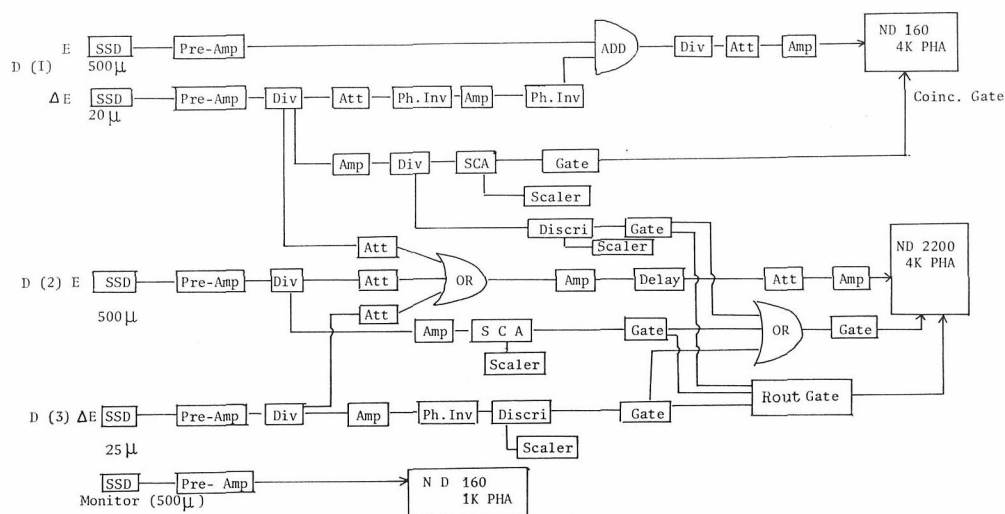M. Yasue, T. Ohsawa, N. Fujiwara, S. Kakigi. D, C. Nguyen, and S. Yamashita

Photo 1: Set up in the scattering chamber.   Three silicon surface
barrier detectors are mounted on the holders.

For the measurement of alpha particles, detectors of 50 μm, 25 μm, and 20 μm depletion depth were used.

On the measurement for the excitation function, three detectors were set at 45°, 115°, and 150° with respect to the beam axis.   The solid angles subtended by the counters were of 0.4, 1.1, and 1.7 m sr, respectively.   The incident proton energy was changed from 4.0 MeV to 6.0 MeV in 50 keV or 100 keV steps.

On the measurement for the angular distributions, detectors on the arm consisted of 20 μm and 1000 μm counter telescope, and on the turn table, two detectors of 500 μm and 25 μm thickness were set 10 degrees apart from each other.   A monitor counter of 500 μm depletion depth was set at the angle of 150 degree.

Protons and deuterons were detected with the 20 μm-1000 μm counter telescope and the 500 μm detector.   At the same time alpha particles were detected with thin detectors of 20 μm and 25 μm thickness.

Block Diagram of Electric Circuit System

Fig. 3.   The electric circuit diagram.

M. Yasue, T. Ohsawa, N. Fujiwara, S. Kakigi. D, C. Nguyen, and S. Yamashita
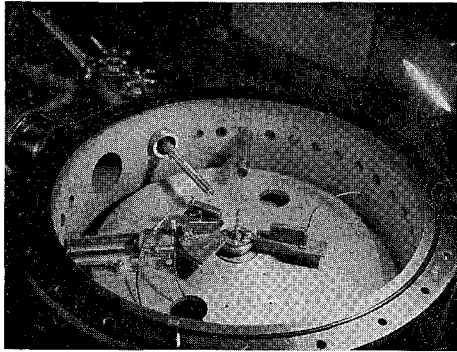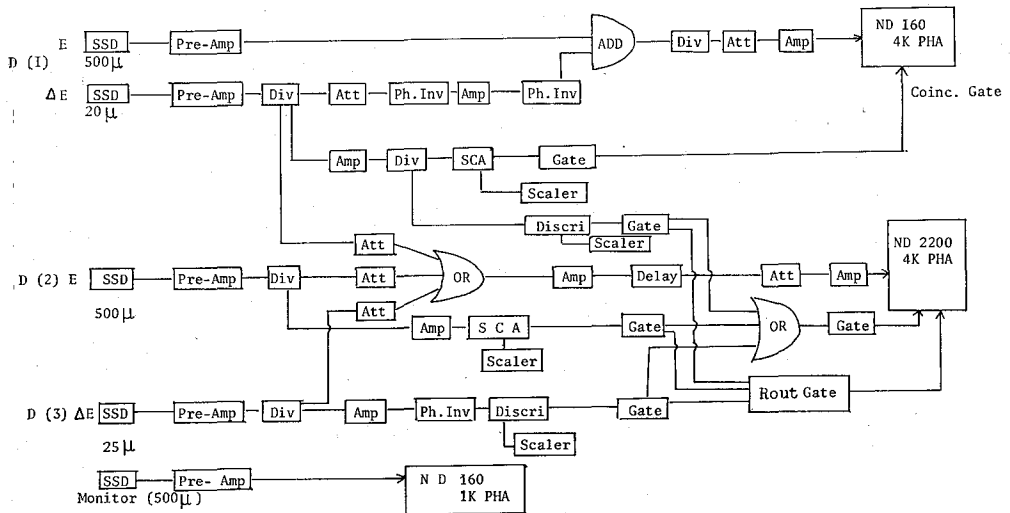

Photo 1:   Set up in the scattering chamber.   Three silicon surface
barrier detectors are mounted on the holders.

For the measurement of alpha particles, detectors of 50 μm, 25 μm, and 20 μm depletion
depth were used.

On the measurement for the excitation function, three detectors were set at 45°,
115°, and 150° with respect to the beam axis.   The solid angles subtended by the counters
were of 0.4, 1.1, and 1.7 m sr, respectively.   The incident proton energy was changed
from 4.0 MeV to 6.0 MeV in 50 keV or 100 keV steps.

On the measurement for the angular distributions, detectors on the arm consisted
of 20 μm and 1000 μm counter telescope, and on the turn table, two detectors of 500
μm and 25 μm thickness were set 10 degrees apart from each other.   A monitor counter
of 500 μm depletion depth was set at the angle of 150 degree.

Protons and deuterons were detected with the 20 μm-1000 μm counter telescope
and the 500 μm detector.   At the same time alpha particles were detected with thin
detectors of 20 μm and 25 μm thickness.

Block Diagram of Electric Circuit System

Fig. 3.   The electric circuit diagram.

(180)

The signals from the detectors were processed by the circuits shown in Fig. 3 and fed to the pulse height analyzers, ND 160 and ND 2200. Over all energy resolutions were 40 keV for protons, and 50 to 60 keV for alpha particles. Angular distributions were measured from 20 degrees to 160 degrees in steps of 5 degrees.

In the present experiment, in order to detect the outgoing particles such as protons, deuterons and alpha particles, the next attentions have been paid.

1. to prepare thin ^{9}Be target in order to lessen energy losses of alpha particles in the target.
2. to identify protons and alpha particles each other. Over the energy range studied, kinetic energy of outgoing protons are too small to use the $\Delta E - E$ counter telescope method. Hence protons were discriminated by stopping background particles with an Al foil of suitable thickness.
3. so as to use machine time efficiently, protons and alpha particles were measured simultaneously using a router circuit.

III. RESULTS

Figures 4 and 5 show energy spectra at Ep = 6.0 MeV, $\theta_{lab} = 115°$. In fig. 4, continuous spectra of alpha particles are observed on the lower channel side of the peak for the ^{9}Be $(p, \alpha_1)^6$Li (2.18) reaction. These are break-up alpha particles from ^{6}Li and ^{8}Be. In fig. 5, these low energy alpha particles and lithium ions are deleted due to an Al-foil of 5.4 μm thickness placed in front of the detector. And so one can observe a broad peak for the ^{9}Be $(p, p_3)^9$Be (3.03) reaction.
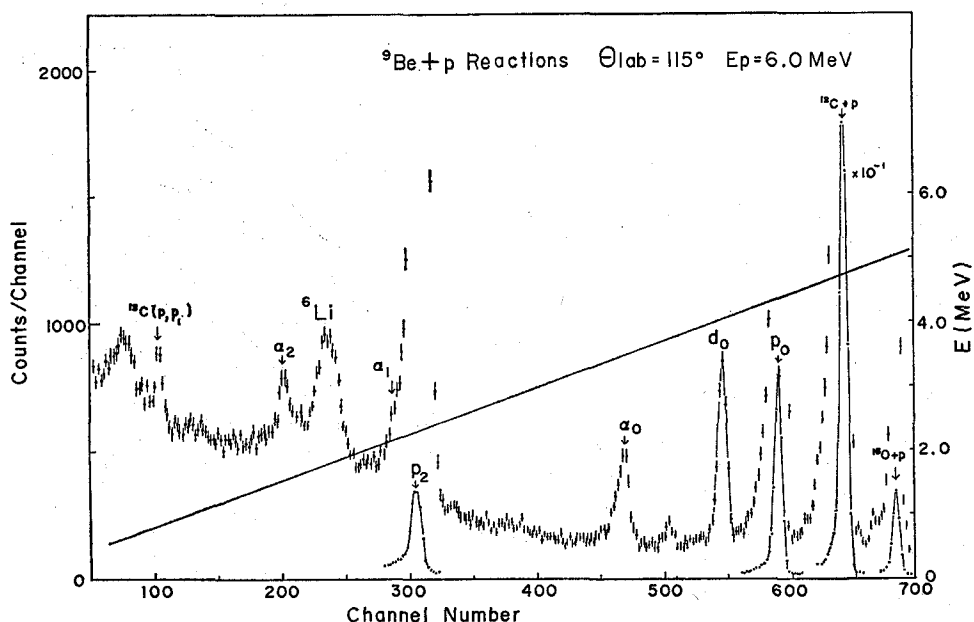

Fig. 4. Typical energy spectrum at $E_p = 6.0$ MeV, $\theta_{lab} = 115°$. The solid line is the energy scale, 7.2 keV/ch. Error bars indicate statistical errors.

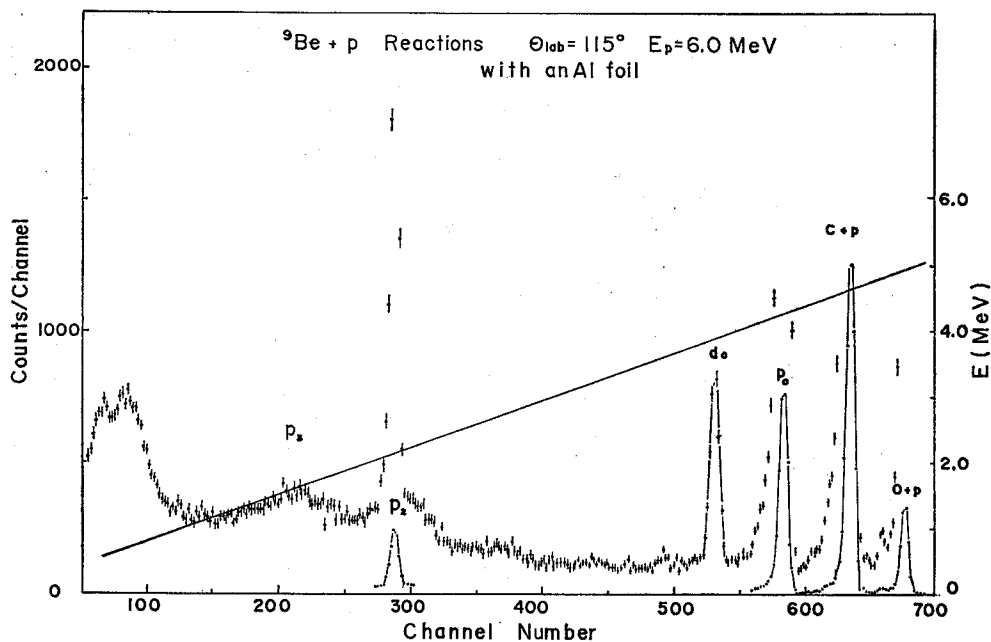Fig. 5. The energy spectrum at $E_p = 6.0$ MeV, $\theta_{lab} = 115°$. An Al-foil of 5.4 μm thickness was mounted in front of the detector. See also caption of Fig. 4.
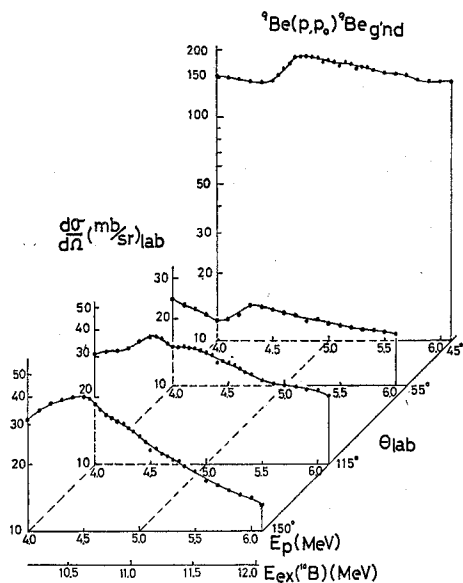

Fig. 6. Excitation functions for the ^{9}Be (p, p_0) ^{9}Be (g'nd) reaction. The ordinates are cross sections in mb/sr in the laboratory system. The abscissa is an incident proton energy in MeV. Errors are within the size of the dots. Solid lines are smooth curves through the data.
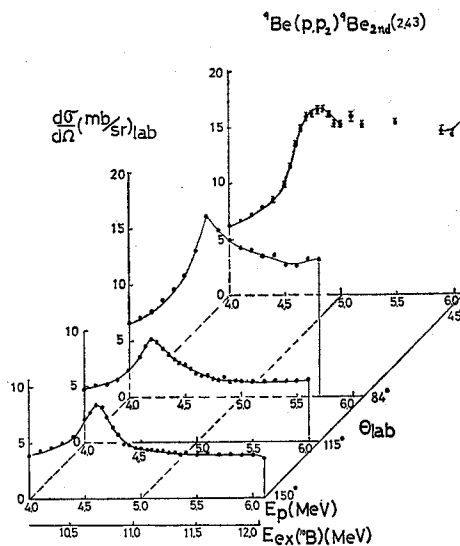

Fig. 7. Excitation functions for the ^{9}Be (p, p_2) ^{9}Be (2.43) reaction. Ordinates are on a linear scale. The blank part in the excitation function at $\theta_{lab} = 45°$ is due to the contamination of Hydrogens.

(182)
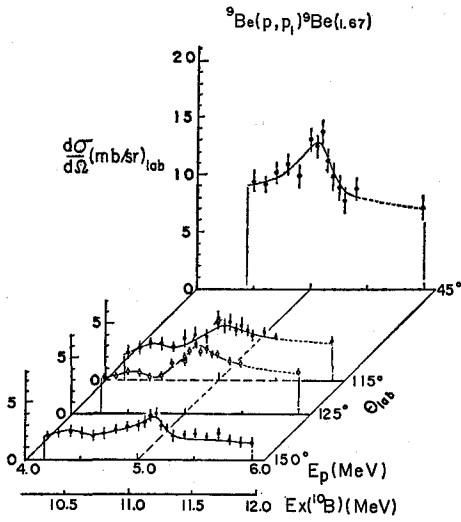
Fig. 8. Excitation functions for the ⁹Be (p, p₁)
⁹Be (1.67) reaction. Error bars denote
statistical errors and ambiguities in
background subtructions.
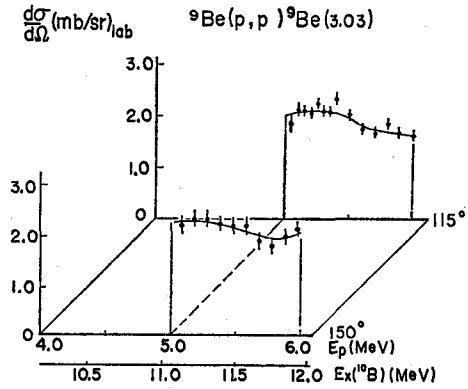
Fig. 9. Excitation functions for the ⁹Be (p, p₃)
⁹Be (3.03) reaction. Below $E_p=5.0$
MeV, the spectrum of p_3 is situated at
the background of alpha particles. So
that only the data above 5 MeV are
shown.

Fig. 10. Excitation functions for the ⁹Be (p, d₀)
⁸Be (g'nd) reaction. Solid lines are
smooth curves through the data.
Broken lines are DWBA calculations
with the code DWUCK.

Fig. 11. Excitation functions for the ⁹Be (p, α₀)
⁶Li (g'nd) reaction.

(183)

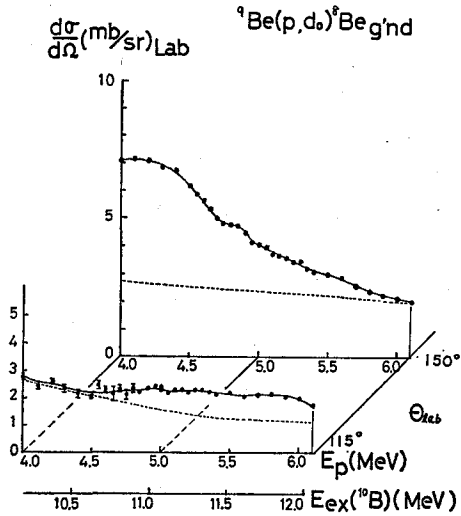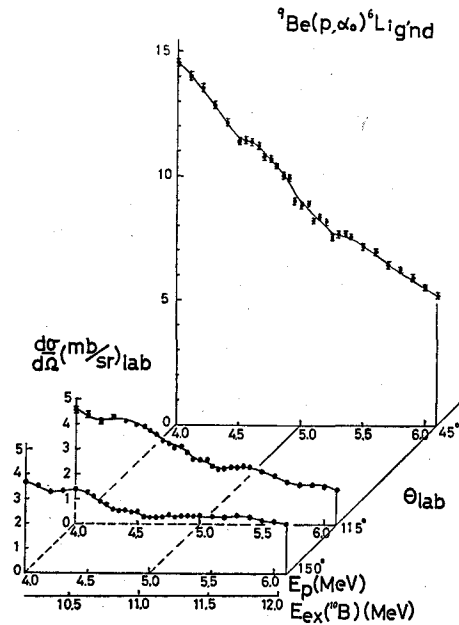M. YASUE, T. OHSAWA, N. FUJIWARA, S. KAKIGI, D. C. NGUYEN, and S. YAMASHITA

^{9}Be(p,α_1)^{6}Li(2.18)

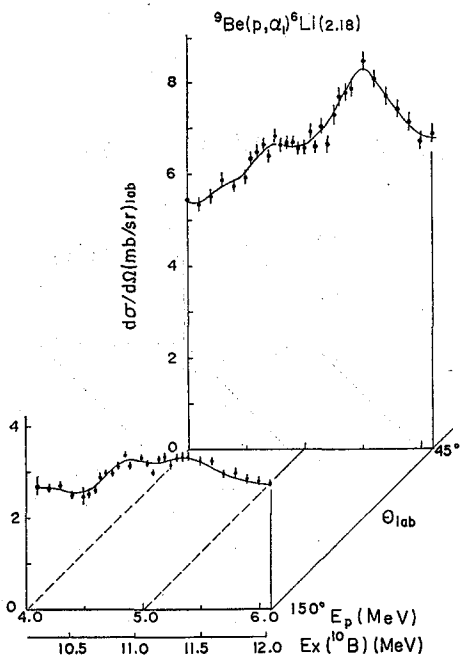

Fig. 12. Excitation functions for the ^{9}Be (p, α_1) ^{6}Li (2.18) reaction. Data at the angle of 115° could not be measured due to the background of ^{6}Li ions.
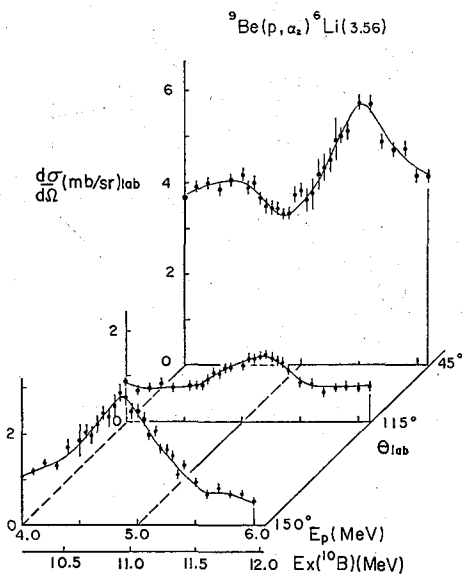
Fig. 13. Excitation functions for the ^{9}Be (p, α_2) ^{6}Li (3.56) reaction.

Figures 6 to 13 show the excitation functions for the proton induced reactions on ^{9}Be at θ_{lab} =45°, 115° and 150°.

In the excitation function for the ^{9}Be(p, p$_0$) ^{9}Be(g'nd) reaction, as seen in Fig. 6, a gross structure is observed near E_p =4.5 MeV (Ex (^{10}B) = 10.6 MeV). In the excitation function for the ^{9}Be (p, p$_2$)^{9}Be (2.43) reaction, as seen in Fig. 7, a resonance with 300 keV width is observed at E_p =4.7 MeV (Ex (^{10}B) =10.8 MeV). In the excitation function for the ^{9}Be (p, p$_1$)^{9}Be (1.67) reaction, as seen in Fig. 8, a resonance like peak is observed at E_p =5.1 MeV (Ex (^{10}B) =11.2 MeV). The excitation function for the ^{9}Be (p, p$_3$)^{9}Be (3.03) reaction, as seen in Fig. 9, is monotonic over the range of proton bombarding energies from 5 MeV to 6 MeV. In the region $E_p \leq 5$ MeV, the energy spectra for p$_3$ are situated at the background of alpha particles. Hence excitation functions for p$_3$ were obtained only over the energy range from 5 to 6 MeV.

In the ^{9}Be (p, d$_0$)^{8}Be (g'nd), and ^{9}Be (p, α_0)^{6}Li (g'nd) reactions, as seen in Figs. 10 and 11, excitation functions are as a whole monotonically decreasing. However, a weak resonance effect is observed at E_p =4.5 MeV (Ex (^{10}B) =10.5 MeV) in the (p, α_0) reaction. In the ^{9}Be (p, α_1)^{6}Li (2.18) and ^{9}Be (p, α_2)^{6}Li (3.56) reactions, as seen in Figs. 12 and 13, excitation functions are complicated and gross peaks are observed at E_p =4.7 MeV (Ex (^{10}B) =10.8 MeV) and E_p =5.5 MeV (Ex (^{10}B) =11.5 MeV).

Figures 14 to 17 show angular distributions for the ^{9}Be (p, p$_2$)^{9}Be(2.43), ^{9}Be (p, α_0)^{6}Li (g'nd), ^{9}Be (p, α_1)^{6}Li (2.18), and ^{9}Be (p, α_2)^{6}Li (3.56) reactions at E_p =4.6, 4.8, and 5.5 MeV. In the (p, α_0) reaction as seen in Fig. 15, the angular distributions

(184)
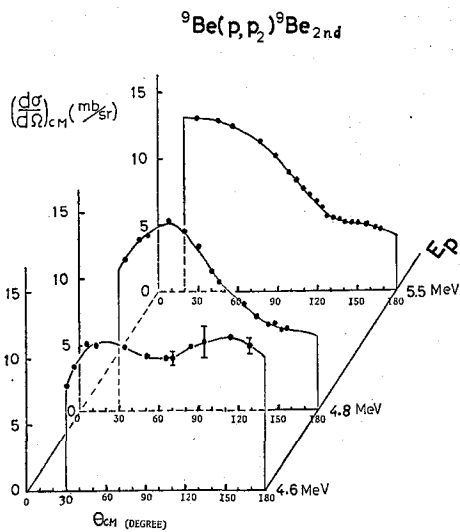
Fig. 14. Angular distributions for the ^{9}Be (p, p$_2$) ^{9}Be (2.43) reaction at E_p=4.6 MeV, 4.8 MeV and 5.5 MeV. The ordinate is cross section in mb/sr in the center of mass system. The abscissa is angle in degrees.
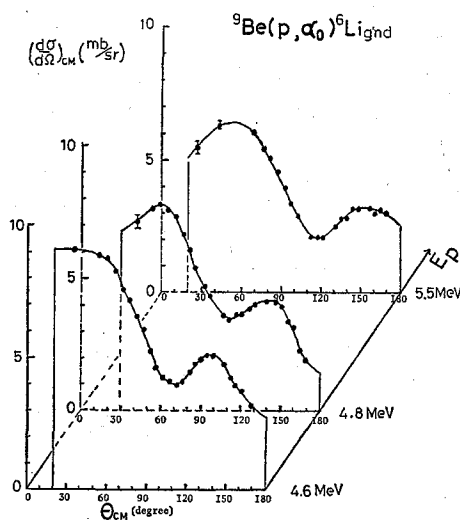
Fig. 15. Angular distributions for the ^{9}Be (p, α_0) ^{6}Li (g'nd) reaction.
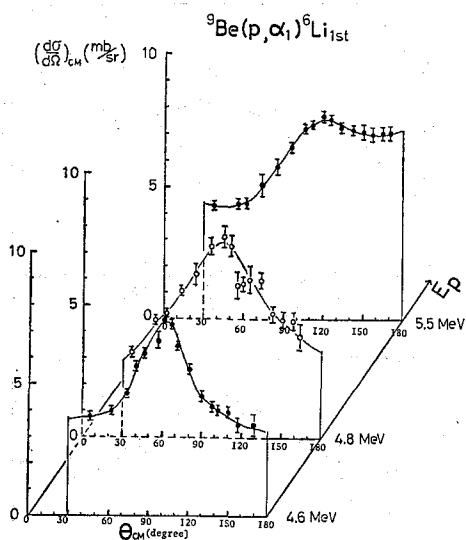
Fig. 16. Angular distributions for the ^{9}Be (p, α_1) ^{6}Li(2.18) reaction.
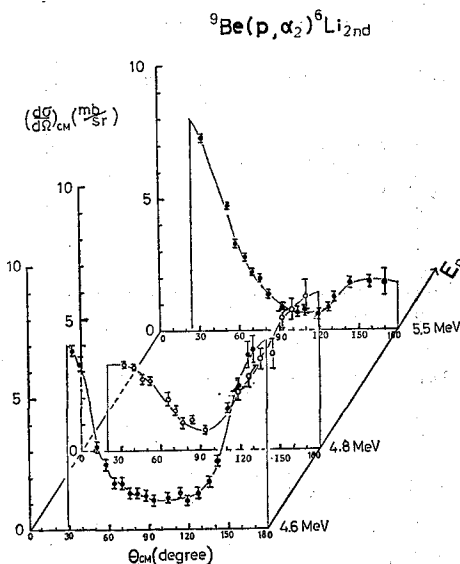
Fig. 17. Angular distributions for the ^{9}Be (p,α_2) ^{6}Li (3.56) reaction.

are similar in shape each other and show diffraction type structure typical of a direct reaction. However, in the (p, p$_2$), (p, α_1), (p, α_2) reactions, as seen in Figs. 14, 16, and 17, angular distributions change in shape with the incident proton energy and show a

resonance effect due to the 10.8 MeV and 11.5 MeV states of ^{10}B. Table I shows the total cross section for the (p, α) reaction. These values are $4\pi A_0$, where A_0 is the zero order coefficient of the Legendre polynominals best fitted to the data. Yields for the (p, α_0), (p, α_1), and (p, α_2) reactions are same order each other.

Table I. Total Cross Section for ^{9}Be $(p, \alpha)^6$Li Reactions in a Unit of mb.

E_p (MeV)	(p, α_0)	(p, α_1)	(p, α_2)
4.6	75.5±1.3	39.0±1.8	27.7±1.3
4.8	69.2±1.8	66.6±1.8	28.3±0.5
5.5		76.6±1.1	32.3±1.0

Figure 18 shows the angular distribution for the ^{9}Be (p, p_2)^{9}Be (2.43) reaction over the range of proton energies from 4.2 MeV to 6.0 MeV. Above $E_p = 5.5$ MeV, angular distributions show forward peaking, but below $E_p = 5.2$ MeV, display falling in forward angles.
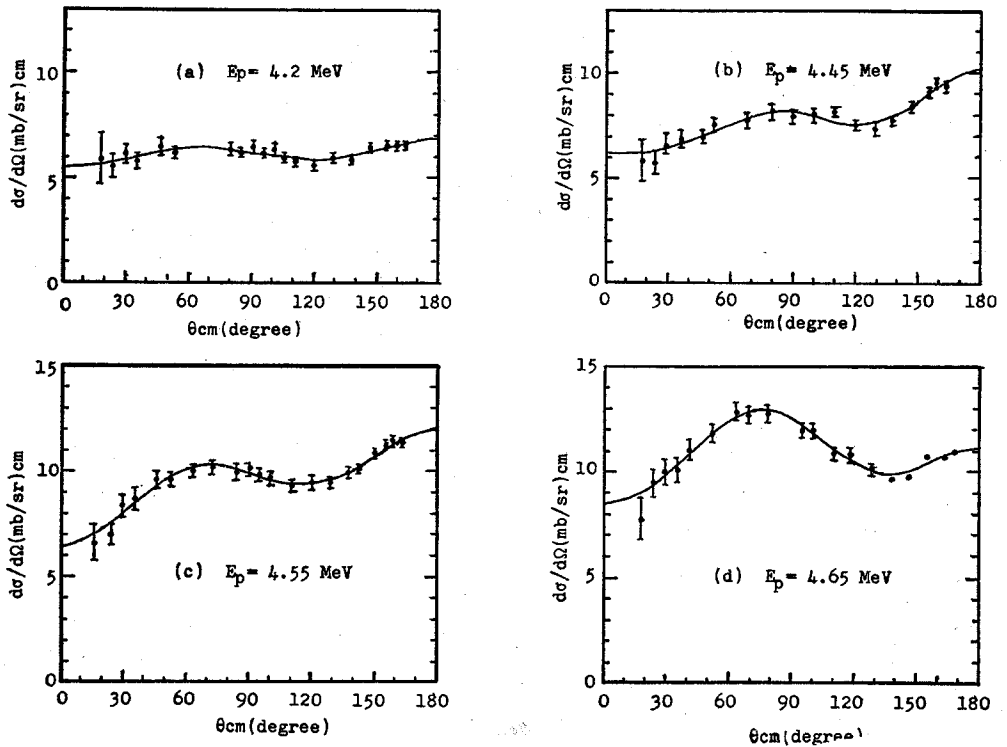
Fig. 18. Angular distributions for the ^{9}Be (p, p$_2$) ^{9}Be (2.43) reaction.
(a) E_p=4.2 MeV, (b) E_p=4.45 MeV, (c) E_p=4.55 MeV, (d) E_p=4.65 MeV,
(e) E_p=4.7 MeV, (f) E_p=4.8 MeV, (g) E_p=5.0 MeV, (h) E_p=5.2 MeV,
(i) E_p=5.5 MeV, (j) E_p=6.0 MeV.
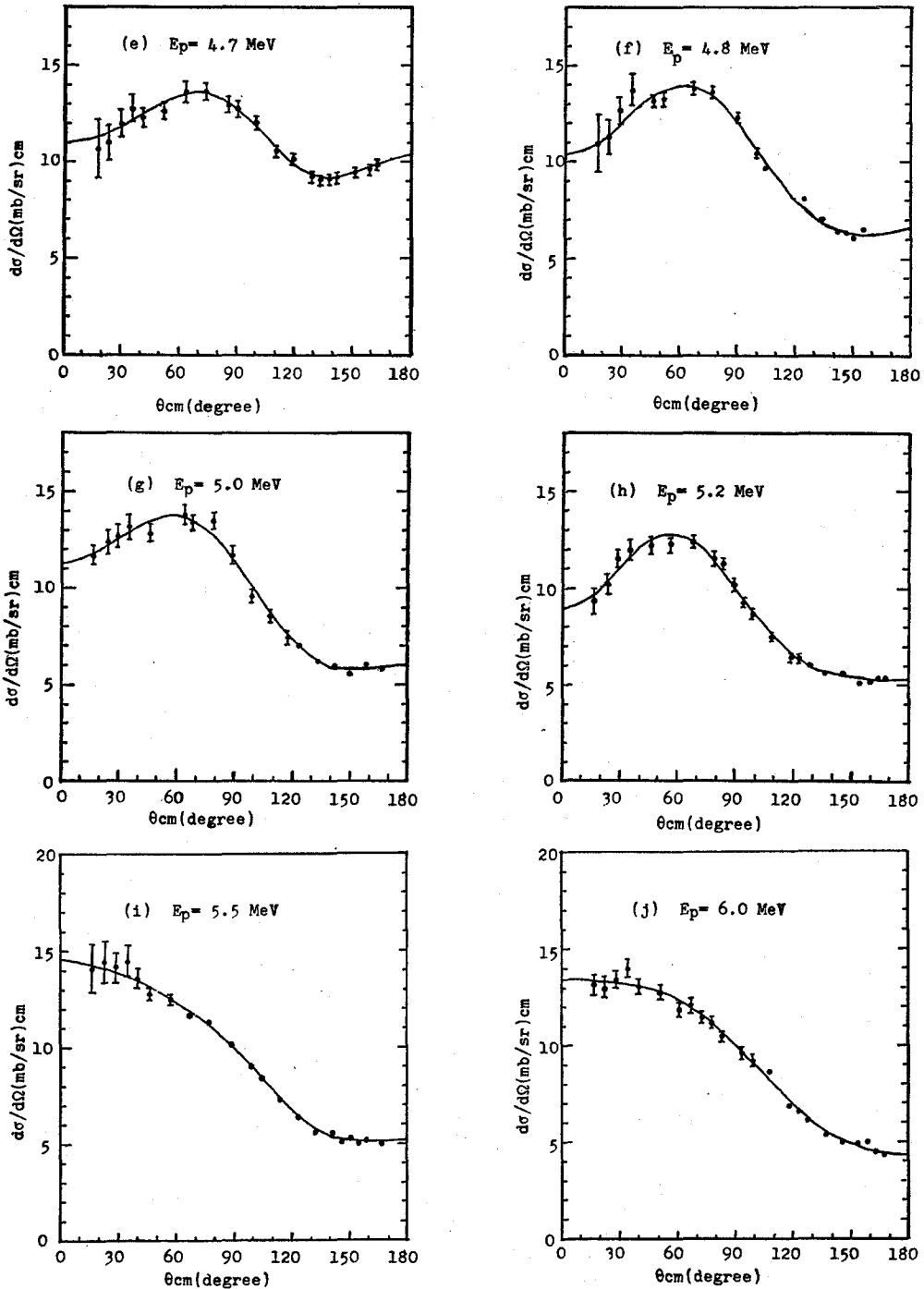Solid curves are the best fit of Legendre function of order 4 to the data. Errors are
smaller than the dots when not shown.

IV. DISCUSSION

The present experiment has been performed with the purpose to find the d* cluster-ing in the excited states in ^{10}B. If the d* clustering can exist in the ^{10}B, it is an essential point that the coupling between the d* clustering and the ^{8}Be core is weak. The interaction between p and n in a $^1S_0$ state is weak and unbound by -50 keV in free space. If the interaction between the p$-$n pair and a ^{8}Be core is strong, the p$-$n pairing in a $^1S_0$ state is broken and cannot form the d* clustering. As stated in the introduction, the strength of the interaction between the p$-$n pair and the ^{8}Be core can be investigated through the ^{9}Be(p, p')^{9}Be* reactions. And the existence of the d* clustering can be searched via the ^{9}Be(p, α_2)^{6}Li (3.56) reaction.

In the excitation function for the ^{9}Be(p, α_2)^{6}Li (3.56) reaction, the 10.8 MeV and 11.5 MeV states of ^{10}B were observed. As discussed above, it is a key-point to the existence of the d* clustering that these states are enhanced also by the proton inelastic channels leading to the positive parity states in ^{9}Be, i.e. ^{9}Be(p, p_1) ^{9}Be (1.67) and ^{9}Be(p, p_3)^{9}Be (3.03) reactions. Experimental results show that the 10.8 MeV state is not observed by the (p, p_1) and (p, p_3) channels, but by the ^{9}Be(p, p_2)^{9}Be* (2.43) channels, and that the 11.5 MeV state is not found in the (p, p') channels. These facts indicate that the 10.8 MeV and 11.5 MeV states in ^{10}B cannot be described in terms of the configuration [^{8}Be core$+$d*] such as expected from the weak coupling model.

Over a range of excitation energies in ^{10}B from 10.2 MeV to 12.0 MeV, the 10.6 MeV, 10.8 MeV, 11.2 MeV, and 11.5 MeV states were observed. The following is the discussions on these states.

(1)   The 10.6 MeV State and the 10.8 MeV State.

Hitherto the 10.8 MeV state in ^{10}B has been studied by many authors[4, 8)] through the ^{9}Be (p, n) and ^{9}Be (p, γ) reactions. Morion et al. observed two peaks near $E_p =$ 4.7 MeV. Similarly in the present experiment two peaks are observed at $E_p =$4.5 MeV (Ex(^{10}B)$=$10.6 MeV) and at $E_p =$4.7 MeV (Ex(^{10}B)$=$10.8 MeV) in the ^{9}Be(p, p_0) reaction, as seen in Fig. 19. Dotted lines in the Fig. 19 are the optical model calcula-tions. Above the dotted lines, one can observe a gross bump with a width of about 1 MeV around $E_p =$4.5 MeV(Ex(^{10}B)$=$10.6 MeV). Usually the broad resonance structures with width of several hundreds keV are interpreted in terms of the "door way" states.[10)] The key-point for the validity of the interpretation in terms of the "door way" states is that the similar broad resonance structures are to appear regularly with a separation energy of several hundreds keV. Other broad resonances such as a width of 1 MeV have not been reported yet on the excited states in ^{10}B. So that another interpretation must be invoked.

The gross peak at $E_p =$4.5 MeV is situated near the threshold energy of 4.65 MeV for the channel, ^{9}Be$+$p$\rightarrow$n$+^9$B(2.33). The fast rising in the yield curves for the ^{9}Be (p, n) reaction at $E_p =$4.5 MeV is ascribed to the effect of the threshold.[8)] At the thresh-old energy, the relative energy between a decaying neutron and a residual nucleus ^{9}B* is small, and long is the time when the neutron stays in the range of nuclear interactions.
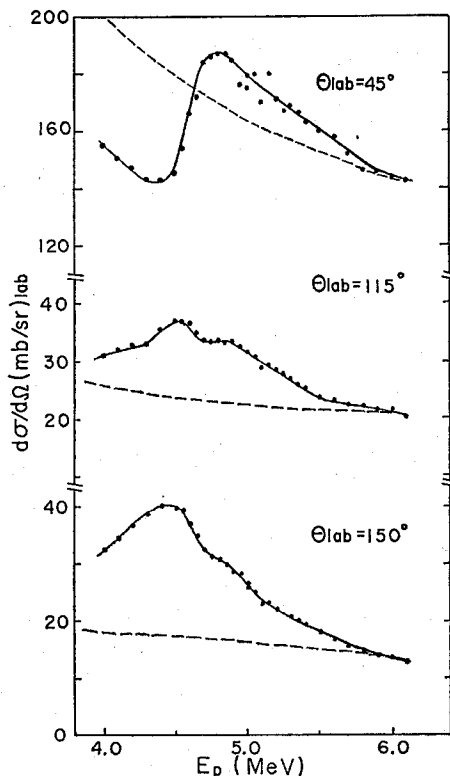
Fig. 19. Excitation functions for the ^{9}Be (p, p$_0$) ^{9}Be (g'nd) reaction. Solid lines are smooth curves through the data. Broken lines are optical model calculations.

Therefore, it is expected that the probability for the ^{9}B(2.33) and n to de-excite into the initial channel, ^{9}Be(g'nd) and p, is large. Namely the anomaly in the elastic scattering at $E_p = 4.5$ MeV is ascribed to the next two step reaction.

$$^9Be + p \rightarrow [^9B(2.33) + n] \rightarrow ^9Be(g'nd) + p .$$
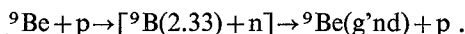
At 1 MeV above the threshold, the time length when the neutron stays in the interaction range is about 3×10^{-22} sec, which is the same order as the interaction time in the direct nuclear reaction. And so the width of the anomaly is reasonable in value. The 2.33 MeV state ^{9}B is analogue to the 2.43 MeV state in ^{9}Be which is the ground state rotational band. The similarity of the structures of ^{9}B(2.33) and ^{9}Be(g'nd) will enhance the probability for the excitation to the ^{9}B(2.33)+n and for the deexcitation to the ^{9}Be (g'nd)+p. Hence it is natural to conclude that the 4.5 MeV anomaly in (p, p$_0$) reaction is due to the above mentioned two step reaction.

As seen in Fig. 11, the 10.6 MeV state is excited weakly in the ^{9}Be(p, α_0)^{6}Li(g'nd) reaction, too. Hence the 10.6 MeV state in ^{10}B is a T=0 state.

The 10.8 MeV state is observed also in the ^{9}Be(p, p$_2$)^{9}Be(2.43) and ^{9}Be(p, α_2) ^{6}Li(3.56) reactions and weakly in the ^{9}Be(p, α_1)^{6}Li(2.18) reaction. The ^{9}Be(p, α_1) ^{6}Li(2.18) and ^{9}Be(p, α_2)^{6}Li(3.56) reactions can excite T=0 and T=1 states, respectively. Therefore, the 10.8 MeV state may be iso-spin impure or doublet.

M. YASUE, T. OHSAWA, N. FUJIWARA, S. KAKIGI, D. C. NGUYEN, and S. YAMASHITA

As stated in Ref. 11, the total cross section for the ^{9}Be(p, p$_2$)^{9}Be(2.43) reaction can be successfully fitted to the one-level formula of Breit-Wigner type, and the analysis with the formula gives a width of 300 keV. Hence one can conclude that the 10.8 MeV state in ^{10}B is a single level of a width of 300 keV, and the iso-spin mixing is due to the tail of the 10.6 MeV state.

Resonance reaction theory predicts that the angular distribution can be expressed by the formula[12]

$$d\sigma/d\Omega = \sum_{L=0}^{K} A_L P_L(\cos\theta), \qquad (1)$$

where L is even, $K = \text{Min } 2(l_i, J, l_f)$.

l_i and l_f are orbital angular momentums in the initial and the final channels, respectively. J is the total angular momentum, $i.e.$ the spin for the intermediate state. In the ^{9}Be (p, α_2)^{6}Li(3.56) $_{j^\pi=0^+, \ T=1}$ reaction, $J = l_{f'}$ and parity is $(-)^{l_f}$. Therefore, J is natural spin parity. According to the possible values of J, values of K are listed in Tables II and III in terms of the (p, p$_2$) and (p, α_2) reactions.

Table II. Possible Values for J, K, l_i, and l_f in the ^{9}Be (p, p_2)^{9}Be (2.43) Reaction.

^{10}B J^π	l_i		l_f		K
	$s_i = 1^-$	$s_i = 2^-$	$s_f = 2^-$	$s_f = 3^-$	
0^+	1			3	0
1^-	0, 2	2	2	2, 4	0 or 2
2^+	1, 3	1, 3	1, 3	1, 3, 5	2 or 4
3^-	2, 4	2, 4	2, 4	0, 2, 4	0, 4 or 6
4^+	3, 5	3, 5	3, 5	1, 3, 5, 7	2, 6 or 8

J^π: total angular momentum, l_i: orbital angular momentum in initial channel, l_f: that in final channel, s_i: channel spin in initial channel, s_f: that in final channel, K: maximum order in the Legendre polynominals,

$$^9\text{Be} + p \rightarrow {}^{10}\text{B} \rightarrow p_2 + {}^9\text{Be (2.43)}$$
$$3/2^- \quad 1/2^+ \quad J^\pi \quad 1/2^+ \quad 5/2^-$$
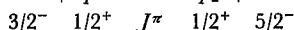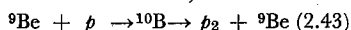
In this case, $s_i = 1^-$ or 2^- and $s_f = 2^-$ or 3^-.

Table III. Possible Values for J, K, l_i, and l_f in the ^{9}Be (p, α_2)^{6}Li (3.56) Reaction.

^{10}B J^π	l_i		l_f	K
	$s_i = 1^-$	$s_i = 2^-$	$s_f = 0^+$	
0^+	1		0	0
1^-	0, 2	2	1	0 or 2
2^+	1, 3	1, 3	2	2 or 4
3^-	2, 4	2, 4	3	4 or 6
4^+	3, 5	3, 5	4	6 or 8

$$^9\text{Be} + p \rightarrow {}^{10}\text{B} \rightarrow \alpha_2 + {}^6\text{Li (3.56)}$$
$$3/2^- \quad 1/2^+ \quad J^\pi \quad 0^+ \quad 0^+$$
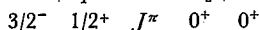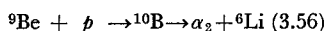
In this case, $s_i = 1^-$ or 2^-, and $s_f = 0^+$.

Angular distributions for (p, p_2) reaction, in Fig. 18, were analyzed in terms of Legendre polynominals up to order four by the method of a least square fit. As shown in Fig. 18, the good fitness of the polynominals to the data means that the order four is sufficient for fitting. Figure 20 shows the coefficients in the Legendre expansions so obtained. Errors shown in Fig. 20 are the probable errors arising from the errors in data and from the difference between the fitted curve and the experimental points. The coefficients A_0 is related to the total cross section (σ) by the formula

$$A_0 = \sigma / 4\pi. \tag{2}$$

Broken lines in Fig. 20 are coefficients in Legendre polynominals fitted to the values calculated with DWBA theory. Normalization of calculated values to the experimental

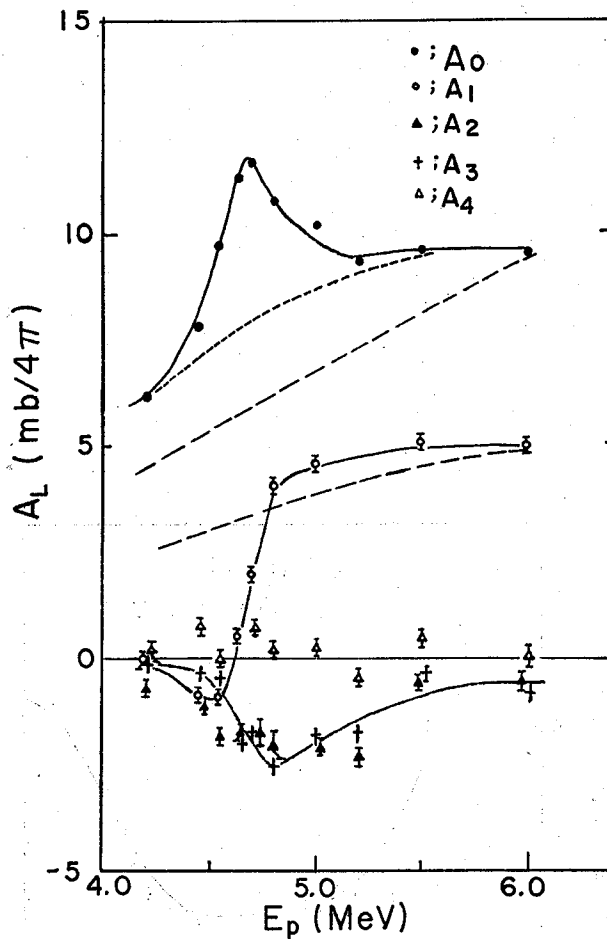

Fig. 20. Energy dependence of the coefficients in Legendre polynominals fitted to the angular distributions for the ^{9}Be (p, p_2) ^{9}Be (2.43) reaction shown in fig. 18. Solid lines are smooth curves through the data. A dotted line denotes values estimated to be continuous background from a fit of the one level formula to the data. Broken lines are DWBA calculations with the code DWBA I.

data were performed at $E_p = 6.0$ MeV in terms of the value of A_0. A dotted line in Fig. 20 is the expected contribution of the direct reaction part, as stated in Ref. 11. The difference between the dotted and the broken curves shows a similar trend as that between data and calculations in the elastic scattering as seen in Figs. 19 and 20. Hence the difference between the expected direct reaction terms and the DWBA calculations can be attributed to the anomaly in the elastic scattering around $E_p = 4.5$ MeV.

Figure 20 indicates that the 4.7 MeV resonance is due to the $L=0$ and $L=2$ terms in the Legendre expansions, and that the variations of the $L=1$ and $L=3$ terms are attributed to the interference between the direct and the resonance reactions. Therefore, one obtains $K=2$, where K is the maximum order in Eq. (1). According to Table II possible values for J^π are 1^-, 2^+ or 4^+.

Figure 21 is the angular distribution for the ^{9}Be(p, α_2)^{6}Li(3.56) reaction at $E_p = 4.6$ MeV, which shows the 90° symmetric shape characteristic of the resonance reaction. So that the data in Fig. 21 was also analyzed in terms of Legendre polynominals. Figure 22 is the variation of chi-squares and A_0 versus the maximun order K in the Legendre expansions. Fit to data indicates $K=4$. According to Table III, possible values for J^π are 2^+ or 3^-. Considering the two cases in the (p, p$_2$) and (p, α_2) reactions, possible values for J^π are limitted to the value of 2^+. Hence one can assign the 10.8 MeV state in ^{10}B to be 2^+.

The following is the consideration on the structure of ^{10}B(10.8).

The total width of the 2.43 MeV state of ^{9}Be is 90% due to p-wave neutron emission to the 2^+ state of ^{8}Be. So that, the 2.43 MeV state of ^{9}Be is interpreted in terms of the configuration of a p-shell neutron coupled strongly to the ^{8}Be(2^+).[20] If so, considering the fact that the 10.8 MeV state of ^{10}B is strongly excited by the ^{9}Be(p, p$_2$)^{9}Be(2.43) reaction, one can propose that the 10.8 MeV state of ^{10}B is a state of a proton and a neutron coupled strongly to the 2^+ state of ^{8}Be. If the 2^+ spin of ^{10}B(10.8) is due to
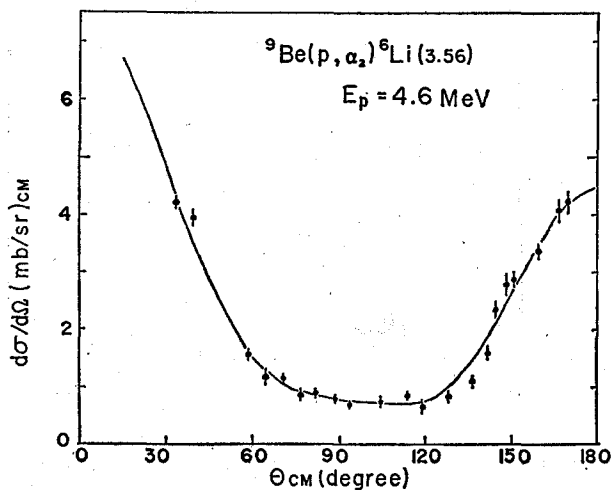

Fig. 21. Angular distribution for the ^{9}Be (p, α_2) ^{6}Li (3.56) reaction at $E_p = 4.6$ MeV. Error bars denote the statistical errors and the ambiguities of background subtractions. The solid line is the best fit of Legendre polynominals of order 4 to the data.
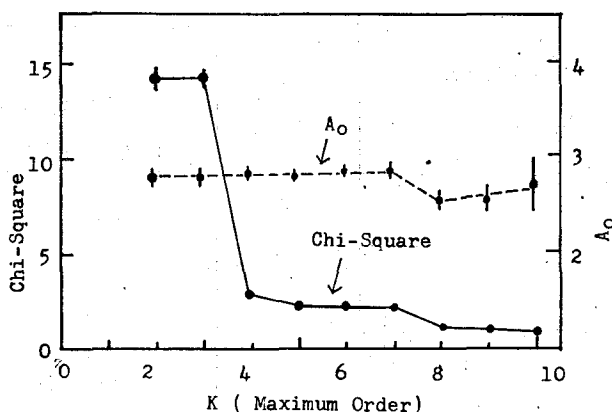
Fig. 22. Variations of chi-square and A_0 versus maximum order K in
Legendre polynominals. A_0 is a coefficient of the zero order
in polynominals. Errors are the probable errors arising from
the errors in data and from the difference between the fitted
curve and the experimental points. Errors are smaller than
the dots when not shown.

the 2^+ spin of the ^{8}Be core, the valence nucleons must couple $S=0^+$ and $T=1$. There-
fore, the proton and the neutron must be in the same orbit each other to couple $S=0$.
The 10.8 MeV state decays also to the α_2+^6Li(3.56) channel, and the ^{6}Li(3.56) is a
state of a proton and a neutron in $1p_{3/2}$ shell coupled to an alpha core. If one assumes
that in the decay of ^{10}B(10.8) to α_2 and ^{6}Li(3.56), the relative wave function between
the proton, the neutron and the alpha is not disturbed so strongly, it is naturally con-
cluded that the 10.8 MeV state of ^{10}B is the configuration of a proton and a neutron
in 1p shell coupled to ^{8}Be(2^+) $i.e.$ [p(1p-shell)+n(1p-shell)+^{9}Be(2^+)] $_{J^\pi=2^+,T=1}$.
As seen in Table II, the fact that the 2^+ state of ^{10}B(10.8) permits the p-wave proton
emission is consisted with the above configuration.

(2)   The 11.2 MeV State in ^{10}B and the ^{9}Be(p, p$_1$) ^{9}Be(1.67) Reaction.

The 11.2 MeV state has been excited only by the ^{9}Be(p, p$_1$)^{9}Be(1.67) reaction.
Angular distributions for the (p, p$_1$) reaction have been measured at $E_p=5.2$ MeV
and 6.0 MeV. As seen in Fig. 23, angular distributions show sharp peaking in forward
angles and flat shapes in backward angles. These structures are similar to Ishiwari's
data at $E_p=6.9$ MeV and 7.3 MeV.[12] The transition of ^{9}Be(g'nd)$_{3/2}$- to ^{9}Be(1.67)$_{1/2}^+$
is produced via the single particle excitation mode $i.e.$ the excitation of a neutron from
the 1p 3/2 shell to the 2s 1/2 shell. In backward angles, the momentum transferred to
a valence neutron is large. Therefore, if one consider the 1.67 MeV state of ^{9}Be
to be an effect of the final state interaction between a neutron in the 1s $_{1/2}$ shell and
a ^{8}Be, the sharp peaking in forward angles is reasonable.

At $E_p=5.2$ MeV, near the resonance energy, the angular distribution doesn't
show resonance like shapes. Therefore, it is expected the 11.2 MeV state is not such
a resonance as described in terms of R-matrix theory.[11]

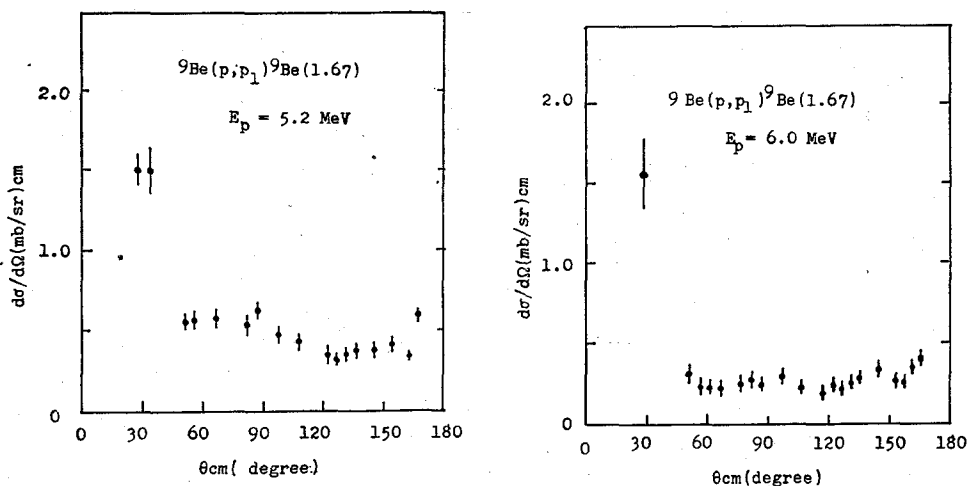As stated in Ref. 13, considerations on the kinematics for the ^{9}Be(p, p$_1$)^{9}Be(1.67)

Fig. 23. Angular distributions for the ^{9}Be (p, p$_1$) ^{9}Be (1.67) reaction.

reaction and analyses with Watson-Migdal theory indicate that the 11.2 MeV state is an effect of overlapping of two body resonances in the $p - n - ^8$Be system.

(3) The 11.5 MeV State in ^{10}B.

The 11.5 MeV state is observed in the ^{11}B(^{3}He, α)^{10}B reaction.[7] In the present experiment, the state was excited also by the ^{9}Be(p, α_1)^{6}Li(2.18) reaction and weakly by the ^{9}Be(p, α_2)^{6}Li(3.56) reaction. Therefore, the 11.5 MeV state is impure in isospin. In the ^{11}B(^{3}He, α)^{10}B reaction, the observed width is 270 ± 50 keV. However, in the ^{9}Be(p, α_1) and (p, α_2) reactions, the width is about 500 keV. The large width in the alpha emitting channels shows that the 11.5 MeV state in ^{10}B has a large alpha particle reduced width. However, the state wasn't observed in the ^{9}Be(p, α_0)^{6}Li(g'nd) reaction.

Figure 24 shows the partial wave scattering amplitudes for the ^{9}Be(p, α)^{6}Li reaction at Ep$=5.5$ MeV. Partial wave amplitudes for the (p, α_1) reaction is one order or two orders greater than those for the (p, α_0), (p, α_2) reactions or those for the (p, p$_0$) scattering, respectively. If one assumes the high spin value such as 4$^+$ for the 11.5 MeV state, it is reasonable that the state cannot be observed in the (p, α_0) and (p, p) reactions.

As seen in Figs. 16 and 17, the angular distributions show complicated shapes which are characteristic of the mixing of several levels. Besides the state is isospin impure. Hence one can conclude that the 11.5 MeV state is not a single level.

(4) Optical Model and DWBA Analyses.

Over the energy range from 5.0 to 6.0 MeV, excitation functions for p$_0$, p$_2$, and d$_0$ are monotonically decreasing functions of energy and the angular distributions for p$_2$ show very little change with energy. These data suggest that the reaction is predominantly a direct process over the energy interval. In order to perform a distorted wave Born approximation (DWBA) calculation, elastic scattering from ^{9}Be was analyzed in terms of optical potential model. The optical potential used had a form of surface absorption type, namely,
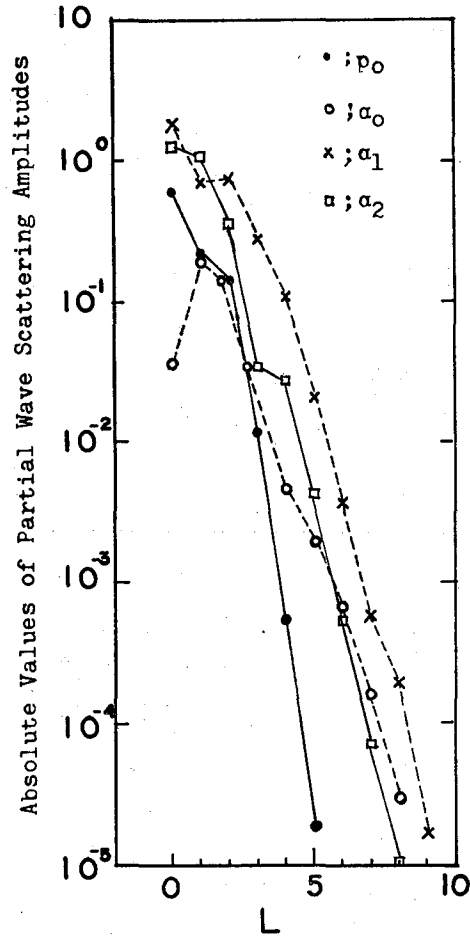
Fig. 24. Variations of the absolute values of partial wave scattering
amplitudes for the ^{9}Be (p, α) ^{6}Li reaction versus the angular
momentum.   Calculations were performed with the code
DWUCK.   Incident proton energy is 5.5 MeV.
p_0: Imaginary part of the amplitudes of $(L+1/2)$ wave for
the ^{9}Be (p, p_0) ^{9}Be. α_0: Real part of the amplitude of L
wave for α_0. α_1: that for α_1. α_2: that for α_2.

$$V = - V_R(r, r_R, a_R) + 4ia_I W_s(d/dr)f(r, r_I, a_I)$$
$$+ \sigma \cdot l V_{so}(\hbar/m_\pi c)^2 (1/r_{so}A^{1/3})(d/dr)f(r, r_{so}, a_{so}) + V_{Coul}(r, r_c), \qquad (3)$$

where f is the usual Woods-Saxon form factor

$$f(r, r_0, a) = \{1 + \exp[(r - r_0 A^{1/3})/a_0]\}^{-1}, \qquad (4)$$

and the Coulomb potential V_{Coul} was that of a uniformly charged sphere, namely,

$$V_{Coul} = (zZe^2/2R_c)(3 - r^2/R_{C^2}), \qquad \text{for} \quad r \leq R_c = r_c A^{1/3}$$
$$= (zZe^2/r), \qquad \qquad \text{for} \quad r > R_c, \qquad (5)$$

z and Z being the charges of the incident and target particles, respectively. The code SEARCH, written by Wada and modified by Koike, was used to perform automatic searches for potential parameters.

Figures 25 and 26 show angular distributions for the elastic proton scattering from ^{9}Be, at $E_p = 6.0$ MeV and 5.0 MeV. These data were cited from Ref. 14. For the 6.0 MeV data, two sets of parameters were obtained. As shown in Table IV, SET 1 represents the best fit to the 6 MeV data and requires a large real potential and small radius. SET 2 are the shallow potential parameter sets. These ambiguities relate well-depth and radius parameters by the formula

$$V_0 R_0^2 \simeq \text{constant}.$$

SET 3, in Table IV, is the best fit to the 5.0 MeV data. As seen in Fig. 26, fitting to the data is worse compared to that at 6.0 MeV. Besides, SET 3 has a large value for the imaginary part. This property in SET 3 is attributed to the effect of a 4.5 MeV bump

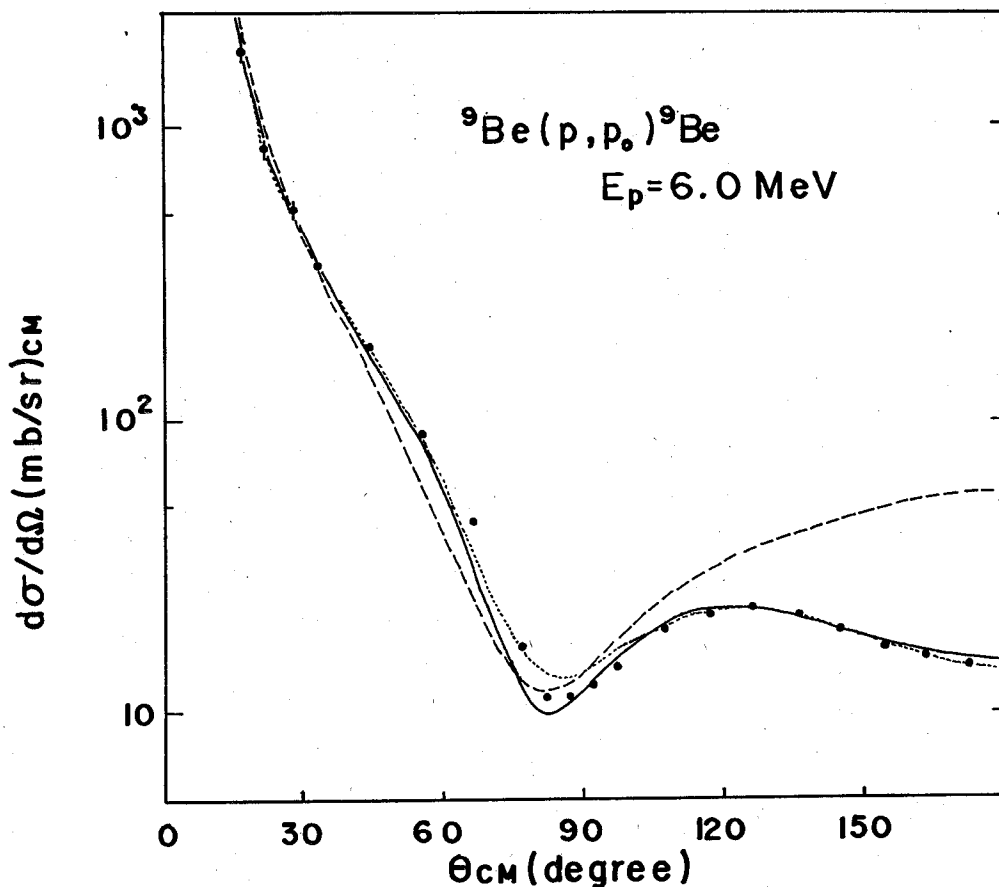Fgi. 25. Angular distribution for the proton elastic scattering from ^{9}Be at $E_p = 6.0$ MeV. Solid curve: optical model calculation with parameters SET 1 in Table IV. Dotted curve: that with SET 2. Broken curve: that with SET 4. Data were cited from Ref. 14.
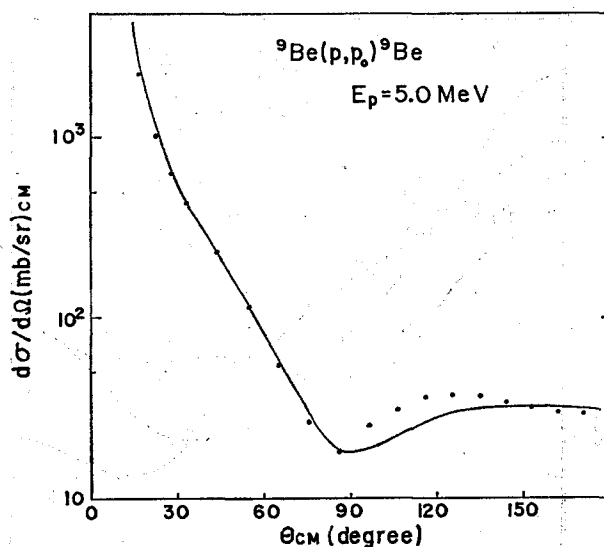
Fig. 26. Angular distribution for the proton elastic scattering from ^{9}Be at $E_p=5.0$ MeV. Solid curve is an optical model calculation with parameters SET 3 in Table IV. Data were cited from Ref. 14.

Table IV. Optical Potential Parameters for Protons and Deuterons.

	SET 1	SET 2	SET 3	SET 4	SET 5
	proton	proton	proton	proton	deuteron
V_R	56.1	41.2	47.6	55.0	84.0
r_R	1.18	1.49	1.18	1.40	1.15
a_R	0.48	0.40	0.78	0.50	0.81
W_s	24.3	21.9	35.8	25.0	15.6
r_s	1.96	1.89	1.96	1.40	1.34
a_s	0.22	0.22	0.22	0.50	0.68
V_{ls}	9.47	5.0	5.25		
r_{ls}	1.18	1.49	1.18		
a_{ls}	0.48	0.40	0.78		
X^2	23.8	72.1	154		

Potentials are surface absorption type.
SET 1, 2, and 4 are at $E_p=6.0$ MeV, SET 3 is at $E_p=5.0$ MeV, and SET 4 is at $E_d=5.0$ MeV.

as shown in Fig. 19. Universal optical potential parameter sets applicable to 1p shell nucleus are reported by Watson et al.[15] SET 1 is similar to Watson's parameter set.

The spectroscopic quadrupole moment of the ground state of ^{9}Be is measured from nuclear magnetic resonance experiments to be $Q_s=3.4$ fm^2.[16] Nillson model calculations predict the deformation of the harmonic oscillator single particle potentials of $\beta \simeq 0.8$ to reproduce the value for Q_s. These facts suggest that ^{9}Be is highly deformed in its ground state. The 2.43 MeV state in ^{9}Be is a member of the ground state rotational band ($K=3/2^-$) and the enhancement of the width of the 2.43 MeV state over
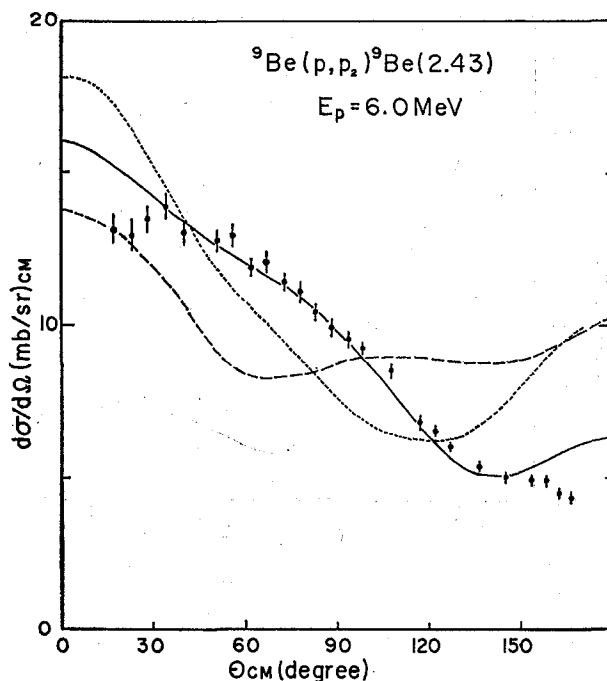
M. YASUE, T. OHSAWA, N. FUJIWARA, S. KAKIGI, D. C. NGUYEN, and S. YAMASHITA

Fig. 27. Angular distribution for the ^{9}Be (p, p$_2$) ^{9}Be (2.43) reaction at E_p=6.0 MeV. Solid curve: DWBA calculation with the code INS–DWBA I. Dotted curve: that with the code DWUCK and with potential parameters SET 1. Broken curve: that with the code DWUCK and with parameters SET 2.

single particle value is approximately 20: 1.[17) Therefore, it is interesting to analyze the ^{9}Be(p, p$_2$)^{9}Be(2.43) reaction with DWBA theory, using a collective-rotational description of ^{9}Be with a $3/2^- - 5/2^-$ spin sequence.

Calculations have been carried out with the code DWUCK, using a collective form factor,

$$F(r) = -[V_R(R_R/a_R)(d/dx_R)f(x_R)],\qquad(6)$$

where f is a Woods-Saxion form factor in Eq. (4). Results of the calculations are presented in Fig. 26. Fits to the data are worse. Tentatively calculations have been retried with the code INS–DWBA I, using the potential parameters SET 4. As shown in Fig. 27, fits to the data are improved. Using the SET 4, calculations have been carried out over the range from 4.0 to 6.0 MeV with DWBA I. The results are shown in Fig. 20. Comparison of calculations with the data gives a deformation β_2 by the formula

$$\beta_2 = (\sigma_{exp}/\sigma_{treor})(1+\delta_{KA,0})(1+\delta_{KB,0})$$
$$*1/[(1+(-)^l)^2 \quad (I_A K_A l 0|I_B K_B)^2(2S_a+1)],\qquad(7)$$

where I_A, I_B, S_a are spins of target nucleus, residual nucleus and incident particles, respectively. K_A and K_B are the projection of the spin on the nuclear symmetry axis. At E_p =6.0 MeV, the formula (7) gives $\beta_2 = 1.6$.

(198)

The large value for β_2 indicates that the coupling between the ground state and the 2.43 MeV state is strong. Hence, the coupled channel analysis is invoked to describe the ^{9}Be(p, p)^{9}Be reaction. Recently Votava et al.[5] calculated coupled channel analyses for the ^{9}Be(p, p)^{9}Be reaction at $E_p = 13$ MeV and gave the deformation $\beta_2 = 1.1$. However, fits to the data are not so improved compared to our results.

In coupled channel equations, a simple Y_{20} deformation is assumed to describe the deformed optical potentials. However, recent Nilsson model calculations on ^{9}Be indicate the necessity for the higher order terms other than Y_{20}, i.e. the sort of deformation which one might envisage for the g'nd-2.43 MeV rotational states is a dumbell of two alpha particles.[18] Hence, in the coupled channel calculations, these higher order terms must be taken into account in terms of the deformed optical potentials.
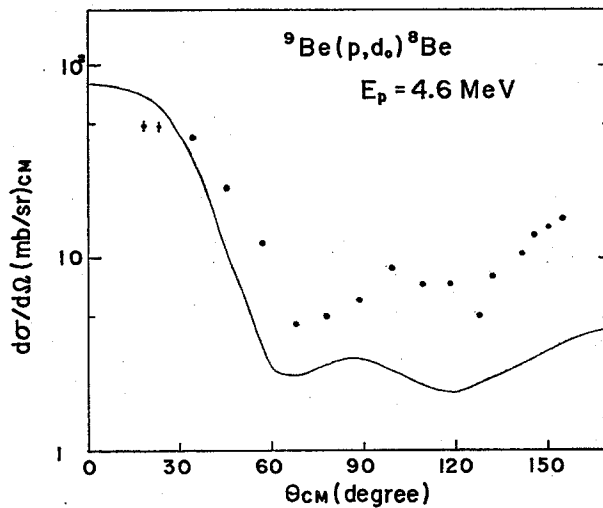

Fig. 28. Angular distribution for the ^{9}Be (p, d$_0$) ^{9}Be (g'nd) reaction at $E_p = 4.6$ MeV.
Dotted curve: Data. Solid curve: DWBA calculation with the code DWUCK,
and potential parameters SET 1 for protons and SET 5 for deuterons.

Figure 28 shows the angular distribution for the ^{9}Be(p, d$_0$)^{8}Be(g'nd) reaction at $E_p = 4.6$ MeV. The binding energy of a neutron in ^{9}Be is -1.67 MeV and smallest in the stable nucleus. Hitherto the ^{9}Be(p, d)^{8}Be reaction has been mentioned as an significant example for the direct reaction process. As seen in Fig. 19, around $E_p = 4.6$ MeV a gross anomaly is observed in the (p, p$_0$) scattering. It is interesting to investigate the effect of the anomaly onto the (p, d) reaction. Hence, the (p, d$_0$) reaction has been analyzed with the DWBA code DWUCK, using the potential parameter SET 1 for protons and SET 5 for deuterons. Parameters for deuterons (SET 5) were deduced from the optical potential formula of Perey's.[19] As seen in Fig. 28, the phase is reproduced. However, the calculated value are small compared to the data. The discrepancies in the absolute value will be attributed to the anomaly in the (p, p$_0$) channel.

M. YASUE, T. OHSAWA, N. FUJIWARA, S. KAKIGI, D. C. NGUYEN, and S. YAMASHITA

Table V. Energy Levels of ^{10}B is a Range of Excitation Energies from 10.2 MeV to 12.0 MeV.

present work					previous works[a]	
E_p (MeV)	E_x (^{10}B) (MeV)	Γ (keV)	J^π, T	decay channels	Γ (keV)	decay channels
4.5	10.6	1 MeV		p_0		
4.5	10.6	200	, 0	p_0, α_0		
4.7	10.8	300	2^+, 1	p_0, p_2, α_2, (α_1)	500	n, α_2
5.1	11.2	300		p_1		
5.5	11.5	500	isospin impure	α_1, α_2	270±50	

(a) See References 4, 7, and 8.

CONCLUSIONS

Excited states of ^{10}B in a range of excitation energies from 10.2 MeV to 12.0 MeV are summarized in Table V. The 10.8 MeV state is $J^\pi = 2^+$, $T = 1$. The configuration of ^{10}B(10.8) has been assinged $[p(p\text{-shell}) + n(p\text{-shell}) + {}^8Be(2^+)]_{J^\pi=2^+,T=1}$. The 11.5 MeV state has a large alpha particle width and is not a single level. The anomaly in the (p, p$_0$) scattering at $E_p = 4.5$ MeV is an effect of the two step reaction, relating strongly to the threshold of the neutron decay. Namely the anomaly is an effect due to a kind of 3 body interaction in the $p - n - {}^8Be$ system. For the further study on the broad anomaly with a width of about 1 MeV, it is hoped for to treat the $^9Be + p$ reaction as a three body system such as the $p - n - {}^8Be$.

ACKNOWLEDGMENTS

REFERENCES

(1) J. C. van der Weerd, T. R. Canada, C. L. Fink, and B. L. Cohen, *Phys· Rev.*, **C3**, 66 (1971).
V. A. Otte, W. von Witsch, J. Sandler, D. Rendic, and G. C. Phillips, *Phys. Rev.*, **C4**, 322 (1971).
W. Bohne, D. Hilscher. H. Homeyer, H. Morgenstern, and J. A. Scheer, *Nucl. Phys.*,

A106, 442 (1968).

(2) B. L. Cohen, E. C. May, T. M. O'Keefe, and C. L. Fink, *Phys. Rev.*, **179**, 962 (1969).
W. Bohne, M. Hagen, H. homeyer, H. Lettau, and J. Scheer, *Phys. Rev. Lett.*, **24**, 1028 (1970).

(3) Yu. A. Kudeyarov, Yu. F. Smirnov, and M. A. Chebotarov, *Sov. J. Nucl. Phys.*, **4**, 751 (1967).
Yu. A. Kudeyarov and R. A. Eramzhyan, *Sov. J. Nucl. Phys.*, **9**, 283 (1969).

(4) J. B. Marion, *Phys. Rev.*, **103**, 713 (1956).
J. B. Marion and J. S. Levin, *Phys. Rev.*, **115**, 144 (1959).

(5) H. J. Votava, T. B. Clegg, E. J. Ludwig, and W. J. Thompson, *Nucl. Phys.*, **A209**, 529 (1973).

(6) L. Grunbaum and M. Tomaselli, *Nucl. Phys.*, **A160**, 437 (1971).
T. Kohmura, private communication.

(7) J. D. Purvis, F. Adjenberg-Selove, and L. M. Polsky, *Phys. Rev.*, **162**, 1005 (1967).

(8) J. B. Marion and Cook, *Phys. Rev.*, **100**, 91 (1955).
J. K. Blair, C. M. Jones, and H. B. Willard, *Nucl. Phys.*, **53**, 209 (1964).

(9) P. Kossanyi-Demay and G. J. Vanpraet, *Nucl. Phys.*, **81**, 529 (1966).

(10) B. Block and H. Feshbach, *Ann. Phys.*, **23**, 47 (1963).

(11) Fay Ajenberg-Selove, "Nuclear Spectroscopy Part B", Academic Press, New York and London, 1960, p. 625.

(12) R. Ishiwari, *Bull. Inst. Chem. Res., Kyoto Univ.*, **39**, 287 (1961).

(13) M. Yasue, to be published in *J. Phys. Soc. Japan.*

(14) F. W. Bingham, M. K. Brussel, and J. D. Steben, *Nucl. Phys.*, **55**, 265 (1964).
M. K. Brussel, private communication.

(15) B. A. Watson, P. P. Singh, and R. E. Segel, *Phys. Rev.*, **184**, 977 (1969).

(16) M. Pomerantz and T. P. Das, *Phys. Rev.*, **119**, 70 (1960).

(17) H. G. Clerc, K. J. Wetzel, and E. Spamer, *Nucl. Phys.*, **A120**, 441 (1968).

(18) A. G. Slight, T. E. Drake, and G. R. Bishop, *Nucl. Phys.*, **A208**, 157 (1973).

(19) C. M. Perey and F. G. Perey, *Nuclear Data Table* **10**, 539 (1972).

(20) R. R. Spencer, G. C. Phllips, and T. E. Young, *Nucl. Phys.*, **21**, 310 (1960).